Egypt. J. Chem. **Vol. 66**, No. 7 pp. 428 - 437 (2023)

Egyptian Journal of Chemistry

http://ejchem.journals.ekb.eg/

TiO_2 Loading on Activated Carbon: Preparation, Characterization, Desulfurization Performance and Isotherm of the Adsorption of Dibenzothiophene from Model Fuel

Burooj Dhia Radhi [a,*], Wadood Taher Mohammed [b]

[a] *Chemical Engineering Department, College of Engineering, University of Baghdad, Baghdad, Iraq*

[b] *Chemical Engineering Department, College of Engineering, University of Baghdad, Baghdad, Iraq*

Abstract

Deep desulfurization of petroleum fuels is an essential requirement to reduce the negative effects of sulfur compounds on the environment and the refining process. Titanium dioxide loading on activated carbon nanoparticles was successfully prepared with two different TiO_2 proportions and introduced as an adsorbent for deep adsorptive desulfurization of dibenzothiophene (DBT) from model fuel via batch adsorption experiments at mild conditions. The prepared adsorbent was characterized by XRD, AFM, BET, SEM, and EDX analysis. The results revealed that the prepared adsorbent is a nanoscale material with an average particle size of 48.9 nm and a large surface area of about 710.12 m^2/g. The adsorbent containing TiO_2 content of 6.33 wt.% achieved a desulfurization efficiency higher than 99% when the initial sulfur concentration in the model fuel was 100 ppm. A high static saturated sulfur capacity of 24.08 (mg S/g adsorbent) was achieved. Equilibrium analysis was investigated with Freundlich, Langmuir, and Temkin isotherm models. Experimental data show the goodness of fitting with Langmuir isotherm and the correlation coefficients (R^2) values were in the order of Langmuir > Freundlich > Temkin.

Keywords: Deep desulfurization; Batch adsorption; TiO_2/activated carbon; Dibenzothiophene

1. Introduction

Sulfur compounds are the most common contaminant that exists in hydrocarbon fuels derived from crude oil such as gasoline, diesel, and jet fuel [1]. Sulfur exists in crude petroleum in different forms with varying quantities, and the concentration of sulfur may range from trace amounts to more than 8 wt.% depending on the crude oils' type and source [2]. Despite its different forms or trace amounts, harmful sulfur compounds act as a serious threat to the environment and public health. The combustion of these compounds releases toxic SO_2 and fine particles resulting in primary environmental pollutants in the air in the form of acid rain, smog, and airborne particulates [3-6]. Moreover, sulfur and its compounds are undesirable in the refining process as they tend to poison expensive catalysts as well as cause corrosion problems in different refining equipment [7-9]. The term 'catalyst poisoning' generally carries an operational definition based on negative interactions between a specific poison (sulfur), catalytic system, and set of reaction conditions [10]. It refers to a decline in the rate of catalytic conversion that may lead to a variation in product selectivity as a result of physically or chemically induced changes in the catalyst [11]. Sulfur may cause significant deactivation even at very low concentrations as it chemisorbs onto and reacts with the active catalyst sites, preventing reactant access and forms strong and stable metal-S bonds that can lead to non-selective side reactions and modify the surface chemistry [12]. In many countries around the world, stringent regulations have been applied to limit the maximum sulfur emissions, for example, the allowable sulfur concentrations in the U.S. have been limited to 30 ppm for gasoline and 15 ppm for highway diesel since 2017 by Environmental Protection Agency (EPA) regulations

*Corresponding author e-mail: b.rahdy0907@coeng.uobaghdad.edu.iq, buroojdrhalh@yahoo.com
EJCHEM use only: Received date 06 December 2021; revised date 06 December 2021; accepted date 05 March 2022
DOI: 10.21608/EJCHEM.2022.109702.5003

[13,14]. Between the years 2013 to 2017, many countries (such as Saudi Arabia, Russia, South Africa, Japan, Hong Kong, Australia, New Zealand, South Korea, Taiwan, and Europe) have permitted a maximum level of sulfur content in gasoline with 10 ppm [2]. Therefore, the desulfurization of hydrocarbon fuels has become one of the most important processes in petroleum refining [15]. Desulfurization processes can be classified according to several aspects, including the hydrogen role (hydrodesulfurization HDS and non-HDS) [16,17], the nature of processes (chemical and/or physical), the treatment method of the organosulfur compounds (decomposed, separated without decomposition or both separated then decomposed) [16], the degree of total sulfur reduction in the refined fuels and cost of the processes [8]. Each desulfurization method applies to specific sulfur compounds and has its advantages and limitations depending on the way how sulfur compounds are transformed [18]. The current main industrial method used to reduce the sulfur level in hydrocarbon fuels is known as hydrodesulfurization (HDS) [18-22]. Although HDS is regarded as a very efficient method in the removal of most aliphatic sulfur compounds such as mercaptans, sulfides, disulfides, and some of the aromatic thiophene derivatives; it is not effective in the removal of alkylated aromatic sulfur compounds such as DBT and its related derivatives under its normal operating conditions due to the steric hindrance and low reactivity of these sulfur compounds. Moreover, the generated H_2S in some of these sulfur compounds' reactions inhibits the HDS [9,14,23]. Due to the remaining of these sulfur compounds in the fuel after the HDS process, they are known as refractory sulfur compounds [23,24]. Recent studies have planned to achieve ultra-deep desulfurization in which little-to-no sulfur fuels or "zero" sulfur fuel (S-content<10 ppm) could be produced. The EPA limit can easily be reached by HDS for lighter fuels such as gasoline, where heavier fuels that contain larger organosulfur compounds cannot be ultra-deep desulfurized effectively by this process [24]. Therefore, other alternatives or supplementary non-HDS techniques have been considered to be sufficient to meet the EPA limits [21,22], including adsorptive desulfurization, extractive desulfurization, bio-desulfurization (BDS), Oxidative desulfurization (ODS), precipitative desulfurization [9], and desulfurization through ionic solutions [25]. Among these promising methods, adsorptive desulfurization (ADS) is regarded as an important, efficient, and most widely used technique which has been intensively studied and described [17,26,27]. ADS can be used to remove sulfur compounds from petroleum-derived fuels in a fixed bed or a batch reactor. Desulfurization via adsorption has several advantages over other techniques based on its capability of direct adsorption of refractory compounds under simple operating conditions of mild temperatures and atmospheric pressure using different solid adsorbent materials. It is an economical process due to its low energy consumption since it does not require costly high-pressure hydrogen reactors or corrosive oxidants making the adsorber design much simpler than other desulfurization techniques discussed before [28, 29]. However, a major challenge for the ADS process is to synthesize adsorbents with high adsorptive capacity, high selectivity to refractory sulfur compounds over other aromatic and olefinic compounds present in the fuel, cost-effective and high regenerability [30]. In this regard, great efforts have focused on the development of novel or modified types of adsorbents. One of the wildly studied adsorbent materials in daily life applications is titanium dioxide (TiO_2), also called titanium oxide or titania, mainly due to its unique properties such as low cost, nontoxicity behavior, high chemical, and physical stability when exposed to acidic and basic compounds, corrosion resistance, superior photocatalytic activity, unique electronic and optical properties, dielectric properties, and biocompatibility [31-33]. Titanium dioxide has six polymorphous of anatase, rutile, brookite, TiO_2-B, TiO_2-H, and TiO_2-II. Among these polymorphs, anatase (with tetragonal structure), rutile (with tetragonal structure), and brookite (with orthorhombic structure) are the main three crystalline phases that have been known to exist in which they represent different arrangements of the TiO_2 crystal structure, their structures are shown in Fig.1. Differences in crystal structures of each type of titanium dioxide induce its different thermodynamic and physical properties such as stability and density. Rutile is considered the most thermodynamically stable phase at normal pressure and room temperature. Both anatase and brookite phases are metastable upon heating and can be converted into rutile phase by calcination processing at ≥550°C [34-37].

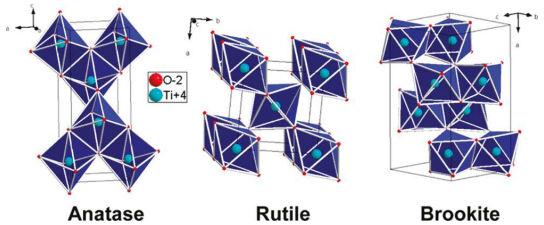

Fig. 1: Representation of TiO_2 different forms [34]

Despite its unique surface effects that ensured good low-temperature desulfurization activity, titania's thermal and mechanical stability is kind of poor. It has been reported that crystalline stability, surface area, and adsorption capacity of TiO_2 could be remarkably enhanced by modification or coupling it with other organic or inorganic materials such as transition metals, zeolites, activated carbon, and mesoporous silica [38,39]. Activated carbons (ACs) are one of the adsorbents which are frequently used for the adsorption of organic compounds in separation and purification applications due to their worthwhile surface properties of large pore volume and high surface area. Despite the high surface area of AC, the use of AC on a large scale is limited because the surface properties do not always have a linear relation with the desulfurization capabilities [21,40]. Moreover, the sulfur capacity of common AC, which is used as an adsorbent for ADS is relatively low, and frequent regeneration is needed. Therefore, it is significantly necessary to increase its sulfur capacity by modification. In previous studies, it is an effective method to improve the desulfurization activity of AC by loading transition metals on its surface such as Cu, Fe, Mn, Ni, and V. Composite materials based on TiO_2 and AC are receiving increasing attention in the field of water treatment. Moreover, TiO_2 could enhance the desulfurization activity of AC even through direct blending [41]. In this regard, the present study reports a simple method to prepare TiO_2 loading on activated carbon nanoparticle adsorbent and evaluate the combined effects of TiO_2 and activated carbon adsorbents for the removal of organosulfur compound dibenzothiophene (DBT) from a model fuel.

2. Experimental section

2.1 Material

All chemicals were used as received without further purification. Titanium isopropoxide, TTIP 98% (Sartort, China); Ethanol 99.8% (Chem-Lab NV, Belgium); powdered activated carbon, AC (BDH, England); Nitric acid, HNO_3 65% (Riedel-de Haen, Germany); n-heptane (Loba- Chemie, India); Dibenzothiophene, DBT 99.1% (Hangzhou Sartort Biopharma, China) and de-ionized water.

2.2 Characterization

X-ray diffraction (XRD) measurements of adsorbent samples were recorded with XRD-6000, Shimadzu, Japan equipped with Ni-filtered CuKα radiation (λ = 1.5418 °A) and operated at 40 kV and 30 mA. The diffractograms were recorded in the range of 2θ from 2° to 80° at a speed rate of 5°/min. The average particle size and topography of the surface of prepared adsorbents were taken by atomic force microscope (AFM). This test shows details about particle size distribution. AFM device type Angstrom, Scanning Probe Microscope, Advanced Inc, AA 3000, USA. Energy-dispersive X-ray spectrometry (EDX) maps attached with Scanning electron microscopy (SEM) measured by Mira3 Tescan, France. Brunauer Emmett and Teller (BET) surface area and pore volume of prepared samples were determined using a system estimated from nitrogen adsorption and desorption by TriStar II Plus.

2.3 Adsorbent preparation

The preparation process of TiO_2 loading on powder-activated carbon nanoparticle adsorbent was as follows: 60 ml of equal volumes mixture of ethanol and deionized water was stirred in a 250 ml conical flask. At first, 5 ml of TTIP was slowly added to the mixture as titanium precursor and the temperature was gradually increased to 78°C with vigorously stirring (1000 rpm) until the solution is completely homogenous. A specific amount of powder-activated carbon (AC) was then introduced while continuing stirring in the presence of HNO_3 to adjust a value of 2–3 of pH solution. After 3 hours of continuous stirring, the composite material was washed and dried at 110°C overnight, followed by calcination at 400°C for 3 hours. TiO_2/activated carbon was characterized with two different proportions based on different amounts of activated carbon. The adsorbent with higher AC content is practically darker. A schematic diagram of the preparation procedure is shown in Fig.2.

2.4 Model fuel

A quantitative amount of DBT was dissolved in n-heptane solvent, such that the sulfur contents of the model fuel samples were 100, 200, 338, and 400 ppm, respectively.

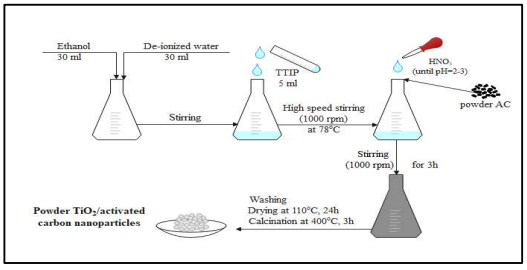

Fig. 2: A schematic diagram of the preparation procedure of TiO_2 loading on powder-activated carbon

2.5 Desulfurization activity testing

All experiments were performed in batch mode under stirred conditions, at atmospheric pressure and room temperature. The experimental procedure was as follows: a specific amount of adsorbent was introduced into a conical flask, the required volume of specific model fuel was poured into the flask containing the weighed adsorbent with oil to the adsorbent ratio of 60, and the fuel was stirred continuously with a magnetic stirrer at constant mixing speed (550 rpm). The adsorption was investigated for different time intervals. Finally, the mixture was filtered with filter papers to separate the adsorbents particles from the solution, and the samples were reserved for sulfur analysis. To calculate the saturation sulfur capacity; 1g of adsorbent was mixed with 90 ml of model fuel with different initial sulfur content in a glass bottle. The mixture was stirred for 48h to reach equilibrium. The sulfur content of fuel samples was determined by ANTEK 9000 N/S analyzer in AL-Dura Refinery/ Ministry of Oil/ Baghdad according to ASTM D-5453 to calculate sulfur content in fuel less than 500 ppm. Each sample was analyzed to calculate the desulfurization efficiency DE% and saturation sulfur capacity q_e (mg S/g adsorbent) according to Eqn. (1) and (2):

$$\text{Desulfurization efficiency\%} = ((C_o - C)/C_o) * 100 \quad (1)$$

$$\text{Saturation sulfur capacity } q_e = (v*(C_o - C))/m \quad (2)$$

Where C_o and C are the initial and final sulfur concentration in fuel (ppm), respectively, v is the volume of liquid fuel sample (liter) and m is the mass of adsorbent [28].

2.6 Adsorption isotherms

As the equilibrium adsorption isotherms describe the relationships between the equilibrium concentration of the adsorbate in the solid adsorbent and the concentration of the adsorbate in liquid fuel at a constant temperature. Single component adsorption isotherms models such as Freundlich [42], Langmuir [43], and Temkin [44] have been employed to fit experimental equilibrium data of DBT adsorption on TiO_2/activated carbon. These isotherm equations can be written as:

$$\text{Freundlich } q_e = K_F C_e^{(1/n)} \quad (3)$$

$$\text{Langmuir } q_e = (q_m K_L C_e)/(1 + K_L C_e) \quad (4)$$

$$\text{Temkin } q_e = B \ln (K_T C_e) \quad (5)$$

Where q_e is the amount of adsorbed sulfur per unit weight of adsorbent at equilibrium (mg S/g adsorbent), C_e is the concentration of adsorbate in the liquid solution associated at equilibrium (mg S/l solution), K_F and n are Freundlich empirical constants which give an indicator of adsorption capacity and adsorption favorability, respectively; q_m is the saturation limit (mg S/g adsorbent); K_L is the Langmuir constant (l/mg); B is the Temkin constant related to the heat of adsorption and K_T is the Temkin isotherm constant. To find the best compatibility between experimental and calculated data from previous isotherms, correlation coefficient R^2 was obtained along with the constants of the three isotherms by non-linear regression analysis.

3. Results and discussions

3.1 Characterization of adsorbent samples

The X-ray diffraction patterns of TiO_2/activated carbon samples with different weight percent of titanium dioxide are shown in Fig.3. Over 2θ range of 20°–80° the diffraction analysis reveals the successful synthesis of TiO_2/activated carbon samples identified by characteristic peaks at 2θ= 25.4°, 37.9°, 48.15°, 53.7° and 55.25° which belong to anatase phase of TiO_2, and the main broad peak at about 2θ=25° being assigned to carbonic material. The crystalline phase of anatase TiO_2 was identified by comparison with the reference data from the International Center for Diffraction Data (JCPDs 21-1272). As the TiO_2 loading on powder-activated carbon was prepared with additional heat-treatment of drying and calcination that did not exceed 110°C and 400°C respectively, the formed anatase phase did not transform into a rutile phase. Although prepared samples include both TiO_2 and AC, the AC peaks cannot be observed clearly because of the higher crystallinity of TiO_2 than AC. So, peaks become broader (as AC is a typical amorphous structure) and diffraction lines intensity decreased as the weight percent of TiO_2 decreased as was expected. Such behavior was also pointed out by [32,41] and [45-47].

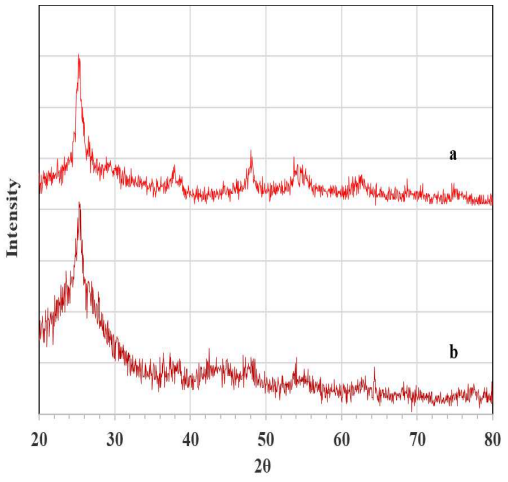

Fig. 3: XRD patterns of TiO_2/activated carbon samples with: (a) Ti content: 35.45 wt. % and (b) Ti content: 6.33 wt.%

The average particle diameter and topography of the TiO_2/AC adsorbent surface have been tested by the atomic force microscope. AFM images allowed a detailed observation of nanometer-size scale at crystal surfaces. The topographical surface images of prepared TiO_2/AC in two-dimensional and three-dimensional are shown in Fig. 4, these images show a uniform nanopore size distribution and the layer growth of the crystal. The cumulative particles size distribution chart shown in Fig. 5 indicates that prepared samples are of nano-size and the average particle size is 48.9 nm.

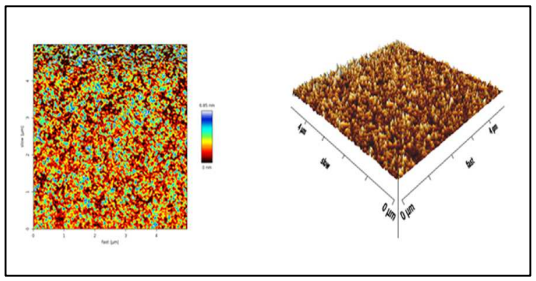

Fig. 4: 2D and 3D AFM images of prepared TiO_2/activated carbon (Ti content: 6.33 wt.%)

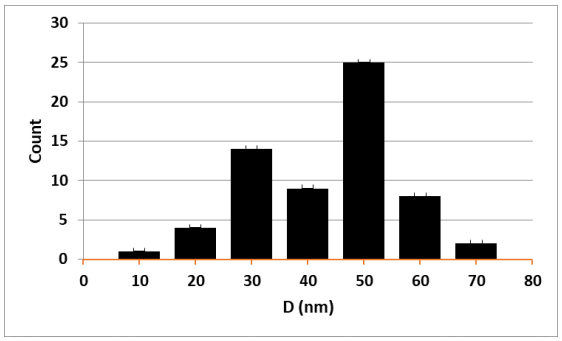

Fig. 5: AFM particles size distribution chart

The values of BET surface area and pore volume of prepared adsorbent are 710.12 m^2/g and 0.464 cm^3/g, respectively. The SEM images and EDX elemental analysis of prepared TiO_2/activated carbon are shown in Fig.6.

As the Scanning electron microscopy (SEM) images give valuable information about surface morphology, the shape and distribution of the TiO_2 particles shown in Fig.6 indicate a non-uniform crystal distribution in which agglomerates on the surface of the activated carbon. Such a result was also pointed out by [32,45]. The EDX elemental mapping analysis of the adsorbent demonstrates the existence of the C element, Ti element, and O element. The TiO_2 low loading content is well evidenced by the EDX microprobe.

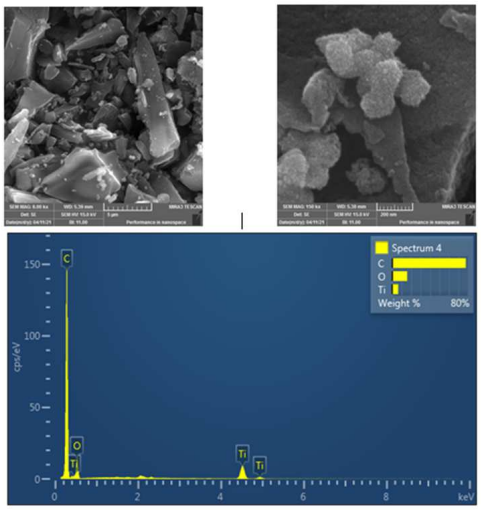

Fig. 6: SEM images and EDX spectra of prepared TiO_2/activated carbon adsorbent (Ti content: 6.33 wt.%)

3.2 Evaluation of desulfurization performance (DE %)

The best removal results were achieved by an adsorbent sample with Ti content of 6.33 wt.%. It can be seen from Table 1, as that the initial sulfur concentration increased (under the same oil to adsorbent ratio conditions), the desulfurization efficiency decreases from nearly a total removal of about 99.79% at an initial sulfur concentration of 100 ppm to reach 65.25% at the initial sulfur concentration 400 ppm. This behavior could be attributed to the high sulfur capacity that permits to adsorb all available amounts of sulfur molecules when there is only 100 ppm until it reaches the maximal capacity of about 24.08 mg S/g adsorbent then it slightly decreases to 23.49 mg S/g adsorbent when initial sulfur content is 400 ppm. This high sulfur content can inhibit the adsorption process due to the lack of direct contact between sulfur molecules and the surface of the adsorbent then both the removal rate and capacity are reduced.

Table 1
Effect of initial sulfur concentration on desulfurization efficiency

Initial sulfur content (ppm)	100	200	338	400
DE (%) at 5h	99.79%	93.08%	79.16%	65.25%
Sulfur capacity (mg S/g adsorbent)	8.98	16.75	24.08	23.49

It was suggested from these results that the sulfur capacity cannot be further increased if the initial sulfur content is increased, and the maximal capacity of the prepared adsorbent is 24.08 mg S/g adsorbent. This high saturation sulfur capacity and high adsorption affinity were attributed to the large surface

area and special structural properties of prepared TiO_2/activated carbon adsorbent. These results with similar behavior can be agreed with [48].

3.3 Adsorption equilibrium analysis (isotherms)

Freundlich, Langmuir, and Temkin isotherms were applied to analyze the experimental data obtained for the removal of DBT from a model fuel with TiO_2/activated carbon adsorbent. Fig. 7, Fig. 8, and Fig. 9 represent the linearized form of eqns. (3), (4), and (5) respectively. The calculated model parameters and correlation coefficients R^2 are shown in Table 2. These results clearly indicate the fitting of experimental data with both Freundlich and Langmuir models as the correlation coefficients are close to unity. However, the best model was the Langmuir model with an R^2 value of 0.998 showing that it is more suitable to describe the presence of a homogenous monolayer of adsorbate at the TiO^2/activated carbon adsorbent surface within the given concentration range. The magnitude of Freundlich coefficient n gives a measure of favorability of the adsorption process. In the range, 2-10 of n values represent good adsorption and an indication of physical adsorption, 1-2 moderately difficult, and less than 1 a poor adsorption [46,47]. This was confirmed with the values of n (6.3938) in the present study which indicates good physical adsorption. According to Langmuir isotherm, the maximum adsorption capacity of DBT on the prepared adsorbent is reported as 24.038 mg S/g adsorbent which is so close to the obtained capacity with an initial sulfur content of 338 ppm. The best analysis of adsorptive desulfurization data by the Langmuir isotherm model was also pointed out by [51] and [52].

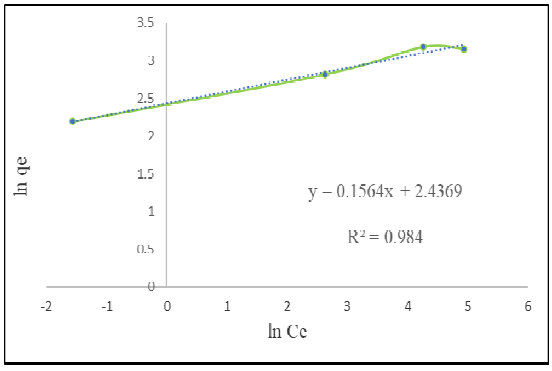

Fig. 7: Freundlich isotherm model for adsorptive desulfurization of DBT on TiO_2/AC adsorbent

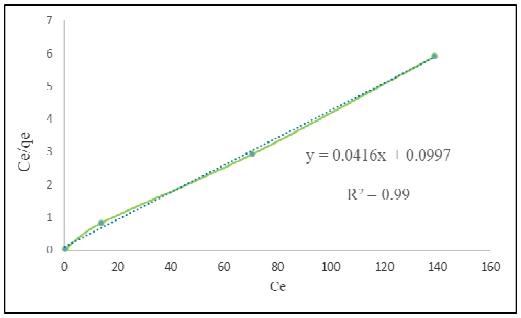

Fig. 8: Langmuir isotherm model for adsorptive desulfurization of DBT on TiO_2/AC adsorbent

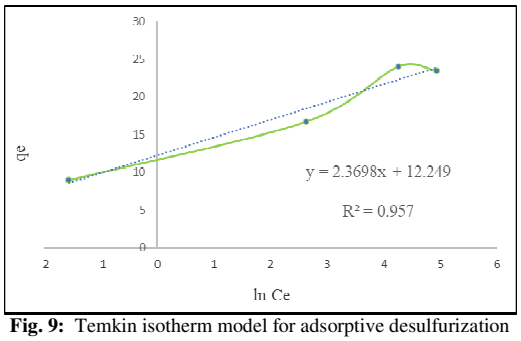

Fig. 9: Temkin isotherm model for adsorptive desulfurization of DBT on TiO_2/AC adsorbent

Table 2
Adsorption isotherm parameters and correlation coefficient of TiO_2/AC adsorbent

Isotherm	Parameter	Value
Freundlich	K_F n R^2	11.4375 6.3938 0.9845
Langmuir	K_L q_m R^2	0.4173 24.038 0.998
Temkin	K_T B R^2	175.7022 2.3698 0.9571

4. Conclusions

TiO_2/activated carbon nanoparticles adsorbent was prepared for the removal of an organosulfur compound DBT from model fuel by batch adsorption process. In this study, the results showed the successful synthesis of nanoscale particles adsorbent with large surface area and good structural properties. Moreover, the prepared adsorbent shows efficient desulfurization performance as excellent removal efficiency and high saturation sulfur capacity at mild conditions. Experimental data have been represented by equilibrium isotherms of Freundlich, Langmuir, and Temkin models. By comparing the correlation coefficients of the models' curves, both Freundlich and Langmuir models are close to unity with a better

description by Langmuir model of a homogenous monolayer coverage of DBT on TiO_2/ activated carbon surface within the given concentration range.

Conflicts of interest

There are no conflicts to declare.

Credit authorship contribution statement

Burooj Dhia Radhi: Methodology, Validation, Investigation, Resources, Data curation, Writing - original draft, Writing – review & Editing, Visualization.

Wadood Taher Mohammed: Conceptualization, Supervision.

Acknowledgment

This work was supported in part by AL-Dura Refinery/ Ministry of Oil/ Baghdad, Iraq. The authors would like to acknowledge the University of Baghdad/ chemical engineering department for assistance and support of this work.

References

[1] P. Sikarwar, V. Gosu, and V. Subbaramaiah, "An overview of conventional and alternative technologies for the production of ultra-low-sulfur fuels," Rev. Chem. Eng., vol. 35, no. 6, pp. 669–705, 2018.

[2] N. S. El-Gendy and H. N. Nassar, "Biodesulfurization in petroleum refining". John Wiley & Sons, Inc., and Scrivener Publishing LLC, USA.1-1179, 2018.

[3] M. A. Hanif, N. Ibrahim, and A. Abdul Jalil, "Sulfur dioxide removal: An overview of regenerative flue gas desulfurization and factors affecting desulfurization capacity and sorbent regeneration," Environ. Sci. Pollut. Res., vol. 27, no. 22, pp. 27515–27540, 2020.

[4] F. Vafaee, S. Mandizadeh, O. Amiri, M. Jahangiri, and M. Salavati-Niasari, "Synthesis and characterization of AFe_2O_4(A: Ni, Co, Mg)-silica nanocomposites and their application for the removal of dibenzothiophene (DBT) by an adsorption process: Kinetics, isotherms and experimental design," RSC Adv., vol. 11, no. 37, pp. 22661–22676, 2021.

[5] D. Singh, A. Chopra, P. K. Mahendra, V. Kagdiyal, and D. Saxena, "Sulfur compounds in the fuel range fractions from different crude oils," Pet. Sci. Technol., vol. 34, no. 14, pp. 1248–1254, 2016.

[6] K. Ennis, "UC Santa Cruz UC Santa Cruz Electronic Theses and Dissertations Title," pp. 1920–2020, 2015, [Online]. Available: https://escholarship.org/uc/item/0jx2107r.

[7] T. A. Saleh, M. N. Siddiqui, and A. A. Al-Arfaj, "Synthesis of multiwalled carbon nanotubes-titania nanomaterial for desulfurization of model fuel," J. Nanomater., vol. 2014, 2014.

[8] M. A. Betiha, A. M. Rabie, H. S. Ahmed, A. A. Abdelrahman, and M. F. El-Shahat, "Oxidative desulfurization using graphene and its composites for fuel containing thiophene and its derivatives: An update review," Egypt. J. Pet., vol. 27, no. 4, pp. 715–730, 2017.

[9] R. Dehghan and M. Anbia, "Zeolites for adsorptive desulfurization from fuels: A review," Fuel Process. Technol., vol. 167, pp. 99–116, 2017.

[10] A. Kolpin et al., "Quantitative Differences in Sulfur Poisoning Phenomena over Ru and Pd: An attempt to deconvolute geometric and electronic poisoning effects using model catalysts," ACS Catal., 2016.

[11] H. Wise, "MECHANISMS OF CATALYST POISONING BY SULFUR SPECIES," in Catalyst Deactivation, C. H. Bartholomew and J. B. Butt, Eds. Amsterdam: Elsevier Science Publishers B.V., 1991, pp. 497–504.

[12] J. Dunleavy, "Sulfur as a Catalyst Poison," Platin. Met. Rev, vol. 50, no. 2, p. 110, 2006.

[13] F. Dheif Ali, "Adsorptive Desulfurization of Liquid Fuels Using Na- Bentonite Adsorbents," Al-Nahrain J. Eng. Sci., vol. 21, no. 2, pp. 248–252, 2018.

[14] T. A. Saleh, K. O. Sulaiman, S. A. AL-Hammadi, H. Dafalla, and G. I. Danmaliki, "Adsorptive desulfurization of thiophene, benzothiophene, and dibenzothiophene over activated carbon manganese oxide nanocomposite: with column system evaluation," J. Clean. Prod., vol. 154, no. October, pp. 401–412, 2017.

[15] P. Gawande and J. Kaware, "Removal of sulphur from liquid fuels using low cost Activated carbon -A review," no. 10, 2016.

[16] H. S. Song, "Desulfurization by Metal Oxide / Graphene Composites," Univ. Waterloo, p. 239, 2014.

[17] S. Wang, R. Wang, and H. Yu, "Deep removal of 4,6-dimethyl dibenzothiophene from model transportation diesel fuels over reactive adsorbent," Brazilian J. Chem. Eng., vol. 29, no. 2, pp. 421–428, 2012.

[18] T. A. Saleh, Applying Nanotechnology to the Desulfurization Process in Petroleum Engineering, vol. i. 2016.

[19] B. A. Abdulmajeed, S. Hamadullah*, and F. A. Allawi, "Deep Oxidative Desulfurization of Model fuels by Prepared Nano TiO_2 with Phosphotungstic acid," J. Eng., vol. 24, no. 11, pp. 41–52, 2018.

[20] G. G. Zeelani and S. L. Pal, "A Review on Desulfurization Techniques of Liquid Fuels," Int. J. Sci. Res., vol. 5, no. 5, pp. 2413–2419, 2016.

[21] D. Jha et al., "Enhanced Adsorptive Desulfurization Using Mongolian Anthracite-Based Activated Carbon," ACS Omega, vol. 4, no. 24, pp. 20844–20853, 2019.

[22] X. U. Cheng-zhi, Z. Mei-qin, C. Keng, H. U. Hui, and C. Xiao-hui, "CeO_x doping on a TiO_2 - SiO_2 supporter enhances Ag based adsorptive desulfurization for diesel," vol. 44, no. 8, 2016.

[23] K. E. Jeong et al., "Selective oxidation of refractory sulfur compounds for the production of low sulfur transportation fuel," Korean J. Chem. Eng., vol. 30, no. 3, pp. 509–517, 2013.

[24] D. T. Tran, J. M. Palomino, and S. R. J. Oliver, "Desulfurization of JP-8 jet fuel: Challenges and adsorptive materials," RSC Adv., vol. 8, no. 13, pp. 7301–7314, 2018.

[25] M. Shakirullah, I. Ahmad, W. Ahmad, and M. Ishaq, "Desulphurization study of petroleum products through extraction with aqueous ionic liquids," J. Chil. Chem. Soc., vol. 55, no. 2, pp. 179–183, 2010.

[26] X. Liang et al., "Synthesis of HKUST-1 and zeolite beta composites for deep desulfurization of model gasoline," RSC Adv., vol. 8, no. 25, pp. 13750–13754, 2018.

[27] T. Adžamić, K. Sertić-Bionda, and M. Mužic, "Kinetic, Equilibrium and Statistical Analysis of Diesel Fuel Adsorptive Desulfurization," Fuels Lubr., vol. 48, no. 3, pp. 384–394, 2009.

[28] M. Ishaq, S. Sultan, I. Ahmad, H. Ullah, M. Yaseen, and A. Amir, "Adsorptive desulfurization of model oil using untreated, acid activated and magnetite nanoparticle loaded bentonite as adsorbent," J. Saudi Chem. Soc., vol. 21, no. 2, pp. 143–151, 2017.

[29] A. Botana-de la Cruz, P. E. Boahene, S. Vedachalam, A. K. Dalai, and J. Adjaye, "Mesoporous Adsorbents for Desulfurization of Model Diesel Fuel: Optimization, Kinetic, and Thermodynamic Studies," Fuels, vol. 1, no. 1, pp. 47–58, 2020.

[30] S. Kumar, N. S. Bajwa, B. S. Rana, S. M. Nanoti, and M. O. Garg, "Desulfurization of gas oil using a distillation, extraction and hydrotreating-based integrated process," Fuel, vol. 220, no. February, pp. 754–762, 2018.

[31] O. L. Kang, A. Ahmad, U. A. Rana, and N. H. Hassan, "Sol-gel titanium dioxide nanoparticles: Preparation and structural characterization," J. Nanotechnol., vol. 2016, no. Table 1, 2016.

[32] C. Orha, C. Lazau, D. Ursu, and F. Manea, "Effect of TiO_2 loading on powder-Activated carbon in advanced drinking-water treatment," WIT Trans. Ecol. Environ., vol. 216, pp. 203–211, 2017.

[33] M. Malekshahi Byranvand, A. Nemati Kharat, L. Fatholahi, and Z. Malekshahi Beiranvand, "A Review on Synthesis of Nano-TiO_2 via Different Methods," J. Nanostructures, vol. 3, no. 1, pp. 1–9, 2013.

[34] D. Dambournet, I. Belharouak, and K. Amine, "Tailored preparation methods of TiO_2 anatase, rutile, brookite: Mechanism of formation and electrochemical properties," Chem. Mater., vol. 22, no. 3, pp. 1173–1179, 2010.

[35] B. A. Abdulmajeed, S. Hamadullah, and F. A. Allawi, "Synthesis and Characterization of Titanium Dioxide Nanoparticles under Different pH Conditions," J. Eng., vol. 25, no. 1, pp. 40–50, 2019.

[36] A. Kumar, "Different Methods Used for the Synthesis of TiO_2 Based Nanomaterials: A Review," Am. J. Nano Res. Appl., vol. 6, no. 1, p. 1, 2018.

[37] E. Y. C. Yan, S. Zakaria, and C. H. Chia, "One-step synthesis of titanium oxide nanocrystal-rutile by hydrothermal method," AIP Conf. Proc., vol. 1614, no. 2014, pp. 122–128, 2014.

[38] H. C.N.C., J. A.A., and T. S., "Synthesis of Zinc Oxide Supported on Titanium Dioxide for Photocatalytic Oxidative Desulfurization of Dibenzothiophene," J. Energy Saf. Technol., vol. 1, no. 1, pp. 1–6, 2018.

[39] L. Rivoira, J. Juárez, H. Falcón, M. Gómez Costa, O. Anunziata, and A. Beltramone, "Vanadium and titanium oxide supported on mesoporous CMK-3 as new catalysts for oxidative desulfurization," Catal. Today, vol. 282, pp. 123–132, 2016.

[40] T. Pedram-Rad, Z. Es'haghi, and A. Ahmadpour, "Adsorptive desulfurization of model gasoline by using modified bentonite," J. Sulfur Chem., vol. 40, no. 2, pp. 149–165, 2018.

[41] C. Zhang, D. Yang, X. Jiang, and W. Jiang, "Desulphurization performance of TiO_2-modified activated carbon by a one-step carbonization-activation method," Environ. Technol. (United Kingdom), vol. 37, no. 15, pp. 1895–1905, 2016.

[42] H.M.F. Freundlich, Over the adsorption in solution, J. Phys. Chem. 57 ,385–470, 1906.

[43] I. Langmuir, The constitution and fundamental properties of solids and liquids, J. Am. Chem. Soc. 38,2221–2295, 1916.

[44] M.J. Temkin, V. Phyzev, Recent modifications to Langmuir isotherms, Acta Physio him. 12, 217–222, 1940.

[45] M. He et al., "Dispersing TiO_2 nanoparticles on graphite carbon for an enhanced catalytic oxidative desulfurization performance," Ind. Eng. Chem. Res., vol. 59, no. 41, pp. 18471–18479, 2020.

[46] M. Li, B. Lu, Q. F. Ke, Y. J. Guo, and Y. P. Guo, Synergetic effect between adsorption and photodegradation on nanostructured TiO_2/activated carbon fiber felt porous composites for toluene removal, vol. 333. Elsevier B.V., 2017.

[47] M. Ouzzine, A. J. Romero-Anaya, M. A. Lillo-Ródenas, and A. Linares-Solano, "Spherical activated carbon as an enhanced support for TiO_2/AC photocatalysts," Carbon N. Y., vol. 67, pp. 104–118, 2014.

[48] L. Zhu et al., "Structure and adsorptive desulfurization performance of the composite material MOF-5@AC," New J. Chem., vol. 42, no. 5, pp. 3840–3850, 2018.

[49] V. O. Shikuku, C. O. Kowenje, and F. O. Kengara, "Errors in Parameters Estimation Using Linearized Adsorption Isotherms: Sulfadimethoxine Adsorption onto Kaolinite Clay," Chem. Sci. Int. J., vol. 23, no. 4, pp. 1–6, 2018.

[50] P. Das, S. Goswami, and S. Maiti, "Removal of naphthalene present in synthetic waste water using novel Graphene /Graphene Oxide nano sheet synthesized from rice straw: comparative analysis, isotherm, and kinetics," Front. Nanosci. Nanotechnol., vol. 2, no. 1, pp. 38–42, 2016.

[51] A. A. Adeyi and F. Aberuaga, "Comparative Analysis of Adsorptive Desulphurization of Crude Oil by Manganese Dioxide and Zinc Oxide," Res. J. Chem. Sci., vol. 2, no. 8, pp. 14–20, 2012, [Online]. Available: www.isca.in.

[52] I. Al Zubaidi, N. N. Darwish, Y. El Sayed, Z. Shareefdeen, and Z. Sara, "Adsorptive Desulfurization of Commercial Diesel oil Using Granular Activated Charcoal," Int. J. Adv. Chem. Eng. Biol. Sci., vol. 2, no. 1, pp. 15–18, 2015.